

Mayer group expansion for solids: application to molecular crystals

E.S. Yakub¹ and L.N. Yakub²

¹*Cybernetics Department, Odessa National Economic University,
8 Preobrazhenskaya Str., Odessa 65082, Ukraine*

²*Thermophysics Department, Odessa National Academy of Food Technologies,
1/3 Dvoryanskaya Str., Odessa 65082, Ukraine*

E-mail: eugene.yakub@gmail.com

Received September 3, 2019, published online December 27, 2019

An approach to evaluation of the Helmholtz free energy using a combination of the Mayer group expansion for molecular crystals and classical Metropolis Monte Carlo method is developed and applied to solid heavy methane CD₄. The location of the phase I–phase II transition line on phase diagram is assessed and compared with existing experimental and computer simulation data.

Keywords: polymorph transition, Monte Carlo, orientation correlations, heavy methane.

1. Introduction

Difficulties in theoretical prediction of the Helmholtz free energy and other related properties (such as entropy or chemical potentials) led to the fact that the most popular methods to obtain the Helmholtz free energy for molecular solids remain Monte Carlo computer simulation [1]. A short overview of the existing theoretical and Monte Carlo simulation methods were presented in our recent paper [2].

Nevertheless even the most sophisticated computer simulation approaches still cannot explain appearance of particular crystalline phases of molecular crystalline solids having certain spatial and orientational structure and their location on the phase diagram, especially at low temperatures.

Recently we proposed a consistent theoretical approach for estimating the Helmholtz free energy for monatomic solids based on the Mayer group expansion technique [2]. It was successfully applied to predicting changes in the properties of highly anharmonic Lennard-Jones crystal along the sublimation and melting line. The comparison with the most precise computer simulation data revealed that theoretical predictions are in excellent agreement with Monte Carlo simulation data in the whole range of temperatures and densities studied.

The purpose of this paper is an attempt to extend the Mayer group expansion technique mentioned above on the simplest molecular solids and test its ability to predict the location of some polymorphic phase transition lines on their phase diagrams.

Extension of the Mayer group expansion technique on molecular solids build from non-spherical molecules is developed in the next section. The method of numerical evaluation of the Helmholtz free energy applied in this work is provided in Sec. 3. As an example of the application object of the proposed approach, we have chosen the phase transition between the orientationally disordered phase I and partially orientationally ordered phase II in the solid CD₄. The corresponding molecular interaction model used in this work is described in Sec. 4.

Results of estimation of this polymorphic transition line location on the phase diagram of CD₄ crystal are discussed and compared with experimental and recent computer simulation data [3] in the final section. Here we discuss the possibility to explain the appearance of certain phases having different orientational and spatial structures in the phase diagram of simple molecular crystals and outline directions for the further development of the theory.

2. Generalization of the Mayer group expansion on molecular solids

We consider below a perfect crystal build from N hard non-spherical molecules at fixed temperature T and volume V . The position and orientation of each molecule is defined by six coordinates: the 3-dimensional radius vector of its center $\mathbf{x}_i = \{x_i^{(1)}, x_i^{(2)}, x_i^{(3)}\}$, and three Euler angles $\omega_i = \{\theta_i, \varphi_i, \psi_i\}$. The potential energy of such crystal is supposed to be a sum of pair potentials:

$$U_N = \sum_{0 < i < j \leq N} \Phi_{ij}(\mathbf{x}_i, \boldsymbol{\omega}_i, \mathbf{x}_j, \boldsymbol{\omega}_j). \quad (1)$$

Following to the Mayer group expansion method proposed earlier [2], the potential energy U_N (1) can be represented as a sum

$$U_N = U_N^{(0)} + \sum_{1 \leq i \leq N} u_1(\Delta \mathbf{x}_i, \Delta \boldsymbol{\omega}_i) + \sum_{1 \leq i < j \leq N} w_{ij}(\Delta \mathbf{x}_i, \Delta \boldsymbol{\omega}_i, \Delta \mathbf{x}_j, \Delta \boldsymbol{\omega}_j), \quad (2)$$

where $U_N^{(0)} = \sum_{0 < i < j \leq N} \Phi_{ij}(\mathbf{x}_i^{(0)}, \boldsymbol{\omega}_i^{(0)}, \mathbf{x}_j^{(0)}, \boldsymbol{\omega}_j^{(0)})$ is the energy of static lattice, $\Delta \mathbf{x}_i = \mathbf{x}_i - \mathbf{x}_i^{(0)}$ are radius vectors of molecular displacements from equilibrium positions $\mathbf{x}_i^{(0)}$, and $\Delta \boldsymbol{\omega}_i = \boldsymbol{\omega}_i - \boldsymbol{\omega}_i^{(0)}$ are deviations of the current molecular orientations from their equilibrium values $\boldsymbol{\omega}_i^{(0)}$ in the static lattice, $u_1(\Delta \mathbf{x}_i)$ are potential energies of single molecules in their static environments referred to their equilibrium positions in the static lattice:

$$u_1(\Delta \mathbf{x}_i, \Delta \boldsymbol{\omega}_i) = \sum_{\substack{1 \leq j \leq N \\ j \neq i}} \left[\Phi(\mathbf{x}_i, \boldsymbol{\omega}_i, \mathbf{x}_j, \boldsymbol{\omega}_j) - \Phi(\mathbf{x}_i^{(0)}, \boldsymbol{\omega}_i^{(0)}, \mathbf{x}_j^{(0)}, \boldsymbol{\omega}_j^{(0)}) \right], \quad (3)$$

and w_{ij} are so-called pair correlation potentials [2]:

$$w_{ij}(\Delta \mathbf{x}_i, \Delta \boldsymbol{\omega}_i, \Delta \mathbf{x}_j, \Delta \boldsymbol{\omega}_j) = \Phi(\mathbf{x}_i, \boldsymbol{\omega}_i, \mathbf{x}_j, \boldsymbol{\omega}_j) - \Phi(\mathbf{x}_i, \boldsymbol{\omega}_i, \mathbf{x}_j^{(0)}, \boldsymbol{\omega}_j^{(0)}) - \Phi(\mathbf{x}_i^{(0)}, \boldsymbol{\omega}_i^{(0)}, \mathbf{x}_j, \boldsymbol{\omega}_j) + \Phi(\mathbf{x}_i^{(0)}, \boldsymbol{\omega}_i^{(0)}, \mathbf{x}_j^{(0)}, \boldsymbol{\omega}_j^{(0)}). \quad (4)$$

Since the molecular crystal is supposed to be mechanically stable, *i.e.*, every single displacement of any molecule from its static position $\mathbf{x}_i^{(0)}$ in the lattice site, and every deviation from the static orientation $\boldsymbol{\omega}_i^{(0)}$ gives an increase in the energy, $u_1(\Delta \mathbf{x}_i, \Delta \boldsymbol{\omega}_i)$ potentials turn to zero when both $\Delta \mathbf{x}_i$ and $\Delta \boldsymbol{\omega}_i$ become zero and are ever non-negative.

Note that according to definition (4) pair correlation potentials w_{ij} will vanish whenever at least one of the interacting atoms enters its lattice site and returns to its equilibrium orientation.

Except the orientational dependence, extension of the approach proposed in [2] on molecular solids requires some generalization which takes into account the possibility of different crystalline structures where molecules may occur

py several types of lattice sites in the lattice having different equilibrium orientations $\boldsymbol{\omega}_i^{(0)}$.

Formally the Mayer group expansion for the Helmholtz free energy remains the same:

$$F_N(V, T) = F_N^{(1)}(V, T) - NkT(W_2 + W_3 + \dots), \quad (5)$$

where $F_N^{(1)}(V, T)$ is the Helmholtz free energy in the Einstein approximation, k is the Boltzmann constant, W_2 and W_3 are, correspondingly, contributions of binary and ternary correlations [2] between the displacements and rotations of molecules.

The Helmholtz free energy in the Einstein approximation

$$F_N^{(1)}(V, T) = F_N^{(\text{id.gas})}(V, T) + U_N^{(0)}(V) - NkT \ln \left(\frac{v_f}{v_0} \right), \quad (6)$$

in turn, includes $F_N^{(\text{id.gas})}(V, T)$; the ideal-gas contribution to the Helmholtz free energy.

Here $U_N^{(0)}(V)$ is the potential energy of the static lattice, v_f is so-called “free volume” per mole, and v_0 is the molar volume unit chosen.

The well-known definition for free volume [4], when applied to molecular crystals depends on the site type, and the corresponding expression must be modified by taking into account existence of s different types of lattice sites.

Integration over molecular positions within the volume v_i ($i = 1, \dots, s$) of the Wigner–Seitz cell must be carried here out along with averaging over all orientations of the selected molecule:

$$v_f(i) = \int_{v_i} \left\langle e^{-u_1(\Delta \mathbf{x}_i, \Delta \boldsymbol{\omega}_i)/kT} \right\rangle_i d\mathbf{x}_i. \quad (7)$$

Here and below the angle brackets denote averaging over all orientations of a molecule within its static environment, and the value of free volume v_f in Eq. (6) must be defined as the average over all s types of the lattice sites:

$$v_f = \frac{1}{s} \sum_{1 \leq i \leq s} v_f(i).$$

Contribution of binary correlations W_2 in Eq. (5) in the case of a molecular crystal depends as well upon both displacements and rotations of molecules and also can be defined as an average over all types of the lattice sites

$$W_2 = \frac{1}{s} \sum_{1 \leq i \leq s} W_2(i).$$

The partial contribution $W_2(i)$, provided that molecule occupies lattice site of i th type, can be written as follows:

$$W_2(i) = \sum_{1 \leq j \leq N} \frac{1}{2Nv_f^{(i)}v_f^{(j)}} \int \int_{v_1 v_j} \left\langle \left\langle \left(1 - e^{-w_{ij}(\Delta \mathbf{x}_i, \Delta \boldsymbol{\omega}_i, \Delta \mathbf{r}_j, \Delta \boldsymbol{\omega}_j)/kT} \right) e^{-[u_1(\Delta \mathbf{x}_i, \Delta \boldsymbol{\omega}_i) + u_1(\Delta \mathbf{x}_j, \Delta \boldsymbol{\omega}_j)]/kT} \right\rangle \right\rangle_{i,j} d\mathbf{x}_1 d\mathbf{x}_j. \quad (8)$$

The expression for contribution of ternary correlations W_3 [2] also can be generalized similarly.

3. Evaluation of the Helmholtz free energy

To test the ability of the theoretical approach presented above to estimate locations of the phase transition lines on the phase diagrams of molecular crystals, we need an efficient method for numerical evaluation of all contributions to the Helmholtz free energy. Numerical procedure of the free energy evaluation in the case of molecular crystals according to Eq. (5) essentially differs from that used for Lennard-Jones solid in Ref. 2.

In this work, we applied a computation scheme which combines different numerical integration methods including Monte Carlo method.

The first relatively simple task is evaluation of the static lattice energy per molecule $u^{(0)}(v) = U_N^{(0)}(V)/N$ for both structures, where $v = V/N$ is molar volume.

Evaluation of the free volume $v_f = v_f(T, v)$ values is a more complicated task. Here we need to calculate the 6-dimensional integral. The following calculation scheme was adopted.

Some basic set of fixed displacements of a molecule center was selected. At each fixed displacement of the molecular center we calculated the value of the integrand in Eq. (7) by averaging it over all orientations of the molecule supposing the distribution over all orientations obeys the Gibbs dis-

tribution and applied the standard Metropolis Monte Carlo technique*.

After performing such calculations for all displacements we approximated the obtained spatial dependence of the integrand in Eq. (7) by a simple analytical function. Taking into account rather low temperatures considered, we applied a kind of quasi-harmonic approximation for the single-particle potential (3):

$$\tilde{u}_1(\Delta \mathbf{x}_i) = \Delta u_i^{(0)} + \sum_{k=1}^3 \sum_{l=1}^3 \alpha_i^{(kl)} \left(\Delta x_i^{(k)} - \delta_i^{(k)} \right) \left(\Delta x_i^{(l)} - \delta_i^{(l)} \right). \quad (9)$$

Approximation (9) contains 10 fitting parameters $\Delta u_i^{(0)}$, $\alpha_i^{(kl)}$, $\delta_i^{(k)}$ ($k, l = 1, 2, 3$) for each type of the lattice position $i = 1, \dots, s$ which can be fitted by minimizing the mean squared deviations of the exponent

$$e^{-\tilde{u}_1(\Delta \mathbf{x}_i)/kT} \quad (10)$$

from the integrand in Eq. (7) averaged over orientations.

After finding values of all parameters $\Delta u_i^{(0)}$, α_{ikl} , δ_{ik} at given T and v it is possible to evaluate the free volume in this approximation for the given lattice site $i = 1, \dots, s$ analytically:

$$\tilde{v}_f(i) = \frac{(\pi kT)^{3/2} e^{-\Delta u_i^{(0)}/kT}}{\sqrt{\left(4\alpha_i^{(11)}\alpha_i^{(22)}\alpha_i^{(33)} - \alpha_i^{(11)}\left(\alpha_i^{(23)}\right)^2 - \alpha_i^{(22)}\left(\alpha_i^{(13)}\right)^2 - \alpha_i^{(33)}\left(\alpha_i^{(12)}\right)^2 + \alpha_i^{(12)}\alpha_i^{(13)}\alpha_i^{(23)} \right)}}$$

and calculate its average over all lattice sites:

$$\tilde{v}_f = \frac{1}{s} \sum_{1 \leq i \leq s} \tilde{v}_f(i). \quad (11)$$

To estimate the contribution of the pair correlation contribution W_2 one must evaluate the 12-dimensional integral (8).

We applied the following calculation scheme. The averaging of integrand in Eq. (8) over orientations of all molecules in the cell was performed using the same Metropolis Monte Carlo technique as in our previous study of CD₄ solid [3].

As in the case of the free volume evaluation, the 6-dimensional spatial dependence of the orientationally averaged integrand in Eq. (8) was approximated as

$$\left(1 - e^{-\tilde{w}(\Delta \mathbf{x}_i, \Delta \mathbf{x}_j)/kT} \right) e^{-[\tilde{u}_1(\Delta \mathbf{x}_i) + \tilde{u}_1(\Delta \mathbf{x}_j)]/kT}. \quad (12)$$

Here $\tilde{w}(\Delta \mathbf{x}_i, \Delta \mathbf{x}_j)$ is an effective pair correlation potential in quasi-harmonic approximation:

$$\tilde{w}(\Delta \mathbf{x}_i, \Delta \mathbf{x}_j) = \Delta w_{ij}^{(0)} + \sum_{1 \leq k, l=3, l \neq k} \beta_{ij}^{(kl)} \Delta x_{ik} \Delta x_{jl}. \quad (13)$$

* The basic set of fixed displacements of a molecule center selected is listed in Table 1.

Table 1. Molecular displacements (in Å) used in calculations

	Δx_1	Δx_2	Δx_3
1	0	0	0
2	0.1	0	0
3	-0.1	0	0
4	0	0.1	0
5	0	-0.1	0
6	0	0	0.1
7	0	0	-0.1
8	0.2	0	0
9	-0.2	0	0
10	0	0.2	0
11	0	-0.2	0
12	0	0	0.2
13	0	0	-0.2
14	0.1	0.1	0.1
15	0.1	-0.1	0.1
16	0.1	0.1	-0.1
17	-0.1	0.1	0.1
18	0.1	-0.1	-0.1
19	-0.1	0.1	-0.1
20	-0.1	-0.1	0.1
21	-0.1	-0.1	-0.1

It should be stressed that here $\Delta w_{ij}^{(0)} \neq 0$ because due to averaging over all orientations this potential does not vanish even when there is no displacements and all molecular centers are in their lattice sites. This obstacle gives the possibility to separate the pure orientational part of the binary correlation contribution:

$$W_2^{(0)} = \frac{1}{2Ns} \sum_{1 \leq i \leq s} \sum_{1 \leq j \leq N} \left(1 - e^{-\Delta w_{ij}^{(0)}/kT} \right).$$

The rest of the binary correlation contribution $W_2^{(1)} = W_2 - W_2^{(0)}$ characterizes the effect of correlations related to molecular displacements. Of course $W_2^{(1)}$ is also affected by orientational correlations and can be evaluated if the remaining 8 parameters $\beta_s^{(kl)}$ ($k, j = 1, 2, 3$) of the effective correlation potential (13) are known.

All the parameters of the effective correlation potential must be obtained for each type of cell sites at all temperatures and molar volumes considered by minimizing the mean squared deviations between orientationally-averaged integrand in Eq. (8) and its quasi-harmonic approximation (12).

Providing that molecule occupies lattice site of i th type ($i = 1, \dots, s$), the contribution of this site type to $W_2^{(1)}$ can be estimated as

$$W_2^{(1)}(i) = -\frac{1}{N} \sum_{\substack{1 \leq j \leq N \\ j \neq i}} \frac{1}{2\tilde{v}_f^{(i)}\tilde{v}_f^{(j)}} \int \int_{v_1 v_j} e^{-[\sum_{k=1}^3 \sum_{l=1}^3 \beta_{ij}^{(kl)} \Delta x_{ik} \Delta x_{jl} + \tilde{u}_1(\Delta \mathbf{x}_i) + \tilde{u}_1(\Delta \mathbf{x}_j)]/kT} d\mathbf{x}_1 d\mathbf{x}_j. \quad (14)$$

Our calculations presented below show that the absolute values of $\beta_s^{(kl)}$ are essentially less than those of $\alpha_i^{(kl)}$ ($k, j = 1, 2, 3$) from Eq. (9). In this case the integrand in Eq. (14) can be replaced by the first non-vanishing term in its expansion in powers of $\beta_s^{(kl)}$ and after averaging over all types of lattice sites we get

$$W_2^{(1)} \approx \frac{1}{16n_s^2} \sum_{i=1}^s \sum_{j=1}^s \sum_{k=1}^3 \sum_{l=1}^3 \frac{(\beta_{ij}^{(kl)})^2}{\alpha_i^{(kk)} \alpha_j^{(ll)}}. \quad (15)$$

This approximate expression was used below in calculations of second contribution to binary correlations, related to molecular displacements.

In order to test the possibility of applying the above approach in predicting locations of the polymorphic phase transitions lines in phase diagrams of simple molecular crystals, we estimated all the above contributions to the Helmholtz free energy of heavy methane CD₄ (phases I and II).

4. Molecular interaction model

In this study, we used the same molecular interaction model as in our recent Monte Carlo simulations of CD₄ crystal [3].

Within this model the pair interaction potential of methane molecules is

$$\Phi_{ij} = \Phi_{CC}(r_{ij}) + \sum_{1 \leq k \leq 4} (\Phi_{CD}(r_{i,jk}) + \Phi_{CD}(r_{j,ik})) + \sum_{1 \leq k, l \leq 4} \Phi_{DD}(r_{ik,jl}) + u_{\Omega-\Omega}(r_{ij}, \boldsymbol{\omega}_i, \boldsymbol{\omega}_j). \quad (16)$$

Here $\Phi_{CC}(r_{ij})$ represents the central interaction of carbon atoms described by the Lennard-Jones (12-6) potential, $\Phi_{CD}(r_{i,jk})$ is short-range atom-atom interaction energy of the carbon atom of i th molecule with k th ($k = 1, \dots, 4$) deuterium atom of j th molecule as a function of the distance $r_{i,jk}$ between these atoms, and $\Phi_{DD}(r_{ik,jl})$ contribution represents interaction of k th deuterium atom of i th molecule and l th deuterium atom of j th molecule as a function of dis-

tance $r_{ik,jl}$ between them. Both C–D and D–D interactions were also represented by the Lennard-Jones (12-6) potential. The internal structure of CD₄ molecules is supposed to be rigid, length of C–D bonds is fixed at $L = 1.095$ Å.

The last term in Eq. (16) $u_{\Omega-\Omega}(r_{ij}, \boldsymbol{\omega}_i, \boldsymbol{\omega}_j)$ represents the octupole-octupole interaction of CD₄ molecules. This contribution supposed to decay with 7th degree of the reciprocal intermolecular distance r_{ij} . Its explicit orientational dependence was adopted from the work of Isnard *et al.* [5].

To reduce the number of model parameters we used the usual Lorentz–Berthelot combination rules:

$$\sigma_{CD} = \frac{1}{2}(\sigma_{CC} + \sigma_{DD}), \quad \varepsilon_{CD} = \sqrt{\varepsilon_{CC}\varepsilon_{DD}}. \quad (17)$$

Details of the potential model calibration could be found in [3], the octupole moment value was adopted from [6]. The model parameters are presented in Table 2.

Table 2. Adopted parameters of the intermolecular interaction potential (16)

Parameter	Value
ε_{DD}/k	8.6 K
σ_{DD}	2.8 Å
ε_{CC}/k	50 K
σ_{CC}	3.63 Å
Ω	$2.3 \cdot 10^{-34}$ esu

5. Results and discussion

We considered the same two cubic CD₄ crystalline structures which were discussed in detail in our previous Monte Carlo simulation study [3]:

- phase I: $s = 4$ (four molecules in the elemental $Fm\bar{3}m$ cell);
- phase II: $s = 8$ (32 molecules in the elemental $Fm\bar{3}c$ cell).

The same two different sizes of the Monte Carlo cell as in our previous paper [3] were used: a “small” one $N = 32$ (160 atoms), and a “large” cell, having twice the size of a “small” cell and containing $N = 256$ molecules (1280 atoms).

In the case of the “small” cell all calculation were performed using cutting radius $R_{\text{cut}} = 5.85$ Å, in the case of the “large” cell R_{cut} was set to 10.0 Å. Results of the static energy minimization for these two sizes of cell and two types of crystalline structures are presented in Table 3. As one can see, at all densities the lattice structure of phase II within the above molecular model has lower static energy than that of phase I.

As it was shown earlier [3], equilibrium properties of both phases in solid CD₄ are determined mainly by short-range intermolecular forces. Therefore we were able to provide averaging over molecular orientations and estimate

free volumes \tilde{v}_f (11) and binary correlation contributions W_2 in both phases I and II using only the “small” Monte Carlo cell (32 molecules).

Table 3. Static energy $u^{(0)}(v)/k$ (in K) for two sizes of the cell

v , cm ³ /mol	$N = 32$		$N = 256$	
	phase I	phase II	phase I	phase II
28.0	–340.7	–400.9	–1298.4	–1359.5
29.0	–445.2	–488.1	–1367.5	–1406.2
30.0	–514.0	–543.3	–1403.2	–1433.7
32.0	–578.6	–590.5	–1408.5	–1421.4

We neglected the ternary W_3 and higher-order correlation contributions, which are important only in highly anharmonic solids [2] and used the minimal symmetric set of molecular displacements (first 13 positions in Table 1). A few tests with the full set of displacements were performed only to estimate the quality of the quasi-harmonic approximations based on the minimal set of molecular displacements. In addition, when calculating W_2 , we took into account only correlations in displacements of nearest neighboring molecules (first coordination sphere).

Evaluation of the Helmholtz free energy of CD₄ solid was performed in phases I and II according to the calculation scheme described above. To be able to compare the results obtained to our previous Monte Carlo simulation data [3] we combined the free volumes and binary correlation contributions computed on the “small” Monte Carlo cell with the energy of static lattice $U_N^{(0)}$ calculated for “large” 256-molecular cell (Table 2).

The main our concern in providing the adopted approach was the problem of estimating many parameters of nonlinear models when minimizing the mean squared deviations between orientationally-averaged integrands in Eqs. (7) and (8) and their quasi-harmonic approximations (10) and (12). To make sure that the values found are correct we used two different numerical methods: Nelder–Mead and Generalized Reduced Gradient algorithms [7], as well as different initial estimates in order to validate the global minimum found. The calculated minima were accepted only if these two methods give the same result.

To estimate the transition line location we computed the excess Helmholtz free energy per molecule $f(v, T) = (F_N - F_N^{\text{id.gas}})/N$ at three temperatures ($T = 30, 35, 40$ K) and four molar volumes ($v = 28, 29, 30,$ and 32 cm³/mol). A rather large number of steps (up to $5 \cdot 10^6$) was required to reach an acceptable accuracy in the course of the Metropolis Monte Carlo averaging of integrands in $v_f(i)$ (7) and $W_2(i)$ (8). Such computations took a large amount of processor time*.

* Evaluation of the Helmholtz free energy at a given temperature and volume for both phases took up to one week of continuous run on 3.4 GHz desktop computer.

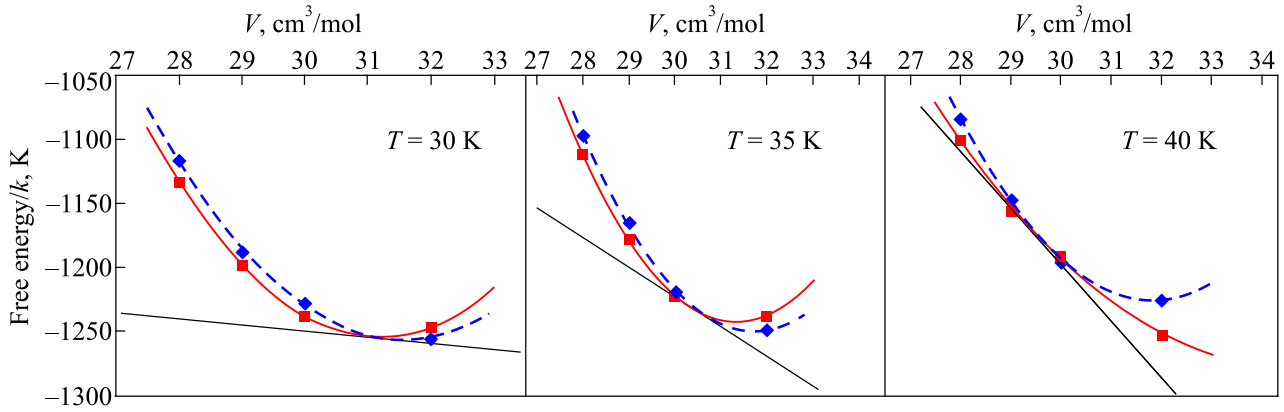


Fig. 1. Volume dependences of the excess Helmholtz free energy in phase I (dashed line) and phase II (solid line) on three isotherms studied. Thin solid lined symbolize common tangents used in determination of the phase transition parameters.

The numerical values of free volumes and correlation corrections obtained as a result of such computations allow us to estimate the role of different contributions to the free energy of both phases. First of all, we made sure that the Helmholtz free energy of phase II in the Einstein approximation (without taking into account correlation contributions), remains lower than that of phase I at all densities and temperatures. Intersection of the Helmholtz free energy isotherms of two phases and transition pressure at a given temperature was obtained only after taking into account the contribution of binary correlations $-kTW_2$.

Analyzing the obtained numerical results on the spatial $W_2^{(0)}$ and orientational $W_2^{(1)}$ contributions to the binary correlation W_2 , we found that their temperature dependence is relatively weak. At the highest densities considered ($v = 28 \text{ cm}^3/\text{mol}$) the spatial contribution $W_2^{(0)}$ in both phases is negative and grows with increasing volume becoming positive at lower densities ($v > 30 \text{ cm}^3/\text{mol}$). The orientational contribution $W_2^{(1)}$, on the contrary, is positive and decreases with decreasing density. Binary correlations are much more important in phase I and lead to a significantly greater decrease in the Helmholtz free energy in this (orientationally disordered) phase.

The numerical values of transition pressures and volumes of coexisting phases were obtained according to the Maxwell rule after approximating the excess Helmholtz free energies of both phases on three isotherms by second-order polynomials as is illustrated in Fig. 1. The results are presented in Table 4 and compared with computer simulation and experimental data in Figs. 2 and 3.

Table 4. Estimated molar volumes of coexisting phases I and II, transition pressures, and the enthalpy of transition

T , K	V_I , cm^3/mol	V_{II} , cm^3/mol	ΔV , cm^3/mol	P , GPa	ΔH , J/mol
30	31.374	31.016	0.358	0.033	385.6
35	30.631	30.316	0.315	0.203	351.7
40	29.67	29.489	0.181	0.353	202.0

As one can see in Fig. 1, the transition pressure, determined by the slope of the common tangent, grows with temperature almost linearly. In Fig. 2 we compare the predicted location of the phase I–phase II transition line with Monte Carlo data obtained earlier [3] using the same potential model (16), (17). The predicted transition temperature at zero pressure is about 28 K.

In Fig. 3 the predicted pressure-temperature relation is compared with locations of transition lines estimated by Stewart [8] and van der Putten [9]. It should be noted that the cell parameters ratio of two phases on the transition line also is in good agreement with experimental data [10,11]. At the same time, the absolute values of both cell parameters differ from experimental data by about 1.5%.

Analyzing the results presented in Table 4, one can see that according to our predictions, phase I–phase II transi-

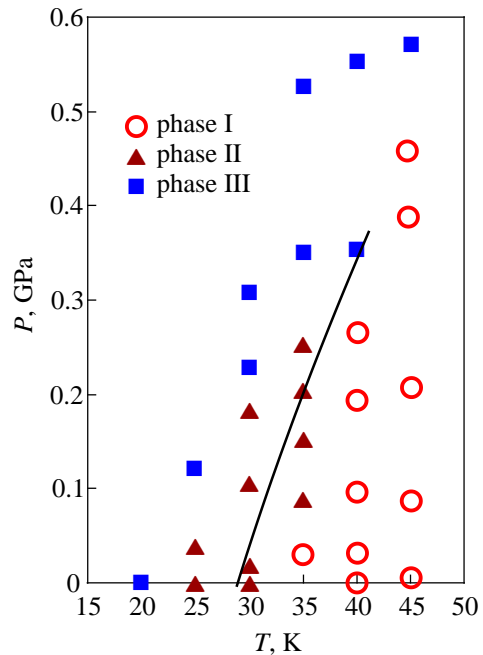


Fig. 2. Comparison of the predicted pressure-temperature dependence of the phase I–phase II transition (solid line) with results of Monte Carlo computer simulation [3].

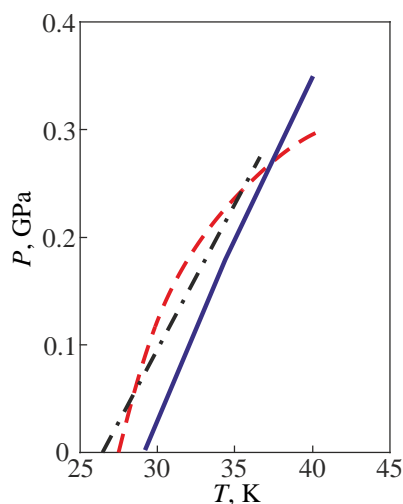


Fig. 3. Comparison of the predicted pressure-temperature dependence of the phase I–phase II transition (solid line) with results of Stewart [8] (dashed line) and van Putten [9] (dash-dotted line).

tion exists up to maximal temperature of $T_{\max} \approx 43\text{--}45$ K, above which this transition disappears (free energy curves do not cross). This result is also in a reasonable agreement with experimental data $T_{\max} \approx 40$ K [8] and $T_{\max} \approx 35$ K [9].

6. Conclusions

In this paper, we presented a new method for estimating the Helmholtz free energy of molecular solids based on the Mayer group expansion technique [2]. As indicated above, the main aim of this work was to test its ability to predict the location of polymorphic phase transition lines on phase diagrams of the simplest molecular solids. This problem recently is increasingly attracting the attention of researchers (see, e.g., [12]).

Surprisingly, despite a number of simplifications made in calculations described above, the predicted location of the CD_4 phase I–phase II transition line agrees well with computer simulation data [3] and properties of coexisting phases are in reasonable agreement with available experimental data [8–11].

These results give us hope that the method proposed may be effective for other types of allotropic phase transitions in molecular crystals, where short-ranged atom-atom forces are responsible for the formation of low-temperature crystalline phases.

At the same time, it should be stressed that there are certain limitations in the use of the applied molecular model. First of all, chemical bonds within this model are rigid and short-range atom-atom repulsion represented by Lennard-Jones (12-6) potentials is too stiff, which limits its applicability at higher temperatures and pressures. Representation of the short-ranged electrostatic interaction only by the octupole-octupole forces is also limited.

It also remains unclear what is the role of ternary W_3 and higher-order correlation contributions to the Helmholtz free energy. According to the results presented above, at last, the differences in the higher-order correlation corrections to the free energy of both phases are small.

Note that there is also a lower temperature limit for the applicability of the proposed approach, since it completely ignores quantum effects. Nevertheless, it is interesting to test the approach proposed in determining the location of other phase transition line (phase I–phase III) in the phase diagram of heavy methane, as well as apply it to other molecular solids like CF_4 , SiH_4 , etc.

1. D. Frenkel, *Understanding Molecular Simulation. From Algorithms to Applications*, 2nd Edition, Elsevier (2002).
2. L. Yakub and E. Yakub, *J. Chem. Phys.* **136**, 144508 (2012).
3. E.S. Yakub, *Fiz. Nizk. Temp.* **45**, 310 (2019) [*Low Temp. Phys.* **45**, 268 (2019)].
4. J.O. Hirschfelder, C.F. Curtiss, and R.B. Bird, *The Molecular Theory of Gases and Liquids*, Wiley, New York (1964).
5. P. Isnard, D. Robert, and L. Galatry, *Molec. Phys.* **31**, 789 (1976).
6. S.M. El-Sheikh, K. Barakat, and N.M. Salem, *J. Chem. Phys.* **124**, 124517 (2006).
7. J.C. Nash, *Compact Numerical Methods: Linear Algebra and Function Minimisation*, Bristol: Adam Hilger (1979).
8. J.W. Stewart, *J. Phys. Chem. Solids* **12**, 122 (1959).
9. D. van der Putten, N.J. Trappeniers, and K.O. Prins, *Physica B* **124**, 193 (1984).
10. E. Legrand and W. Press, *Solid State Commun.* **18**, 1353 (1976).
11. J.G. Aston, Q.R. Stottlemeyer, and G.R. Murray, *J. Am. Chem. Soc.* **82**, 1281 (1960).
12. N.P. Schieber, E.C. Dybeck, and M.R. Shirts, *J. Chem. Phys.* **148**, 144104 (2018).

Груповий розклад Майєра для твердих тіл:
застосування до молекулярних кристалів

Є.С. Якуб, Л.М. Якуб

Розроблено підхід до оцінки вільної енергії Гельмгольца з використанням комбінації групового розкладу Майєра для молекулярних кристалів та класичного методу Монте-Карло для твердого важкого метану. Оцінене положення лінії переходу фаза I–фаза II на фазовій діаграмі CD_4 порівнюється з експериментальними даними та даними комп'ютерного моделювання.

Ключові слова: поліморфний перехід, метод Монте-Карло, орієнтаційні кореляції, важкий метан.

Групповое разложение Майера для твердых тел:
применение к молекулярным кристаллам

Е.С. Якуб, Л.Н. Якуб

Разработан подход к оценке свободной энергии Гельмгольца с использованием комбинации группового разложения Майера для молекулярных кристаллов и классического

метода Монте-Карло для твердого тяжелого метана. Оцененное положение линии перехода фаза I–фаза II на фазовой диаграмме CD_4 сравнивается с экспериментальными данными и данными компьютерного моделирования.

Ключевые слова: полиморфный переход, метод Монте-Карло, ориентационные корреляции, тяжелый метан.